

# Performance Analysis of Downlink MIMO-NOMA Systems Over Weibull Fading Channels

Lenin Patricio Jiménez Jiménez  
Dept. of Communications  
University of Campinas  
Campinas, Brazil  
l264366@dac.unicamp.br

Fernando Darío Almeida García  
Dept. of Communications  
University of Campinas  
Campinas, Brazil  
ferdara@decom.fee.unicamp.br

Maria Cecilia Luna Alvarado  
Dept. of Communications  
University of Campinas  
Campinas, Brazil  
m264371@dac.unicamp.br

Gustavo Fraidenraich  
Dept. of Communications  
University of Campinas  
Campinas, Brazil  
gf@decom.fee.unicamp.br

Michel Daoud Yacoub  
Dept. of Communications  
University of Campinas  
Campinas, Brazil  
mdyacoub@unicamp.br

José Cândido S. Santos Filho  
Dept. of Communications  
University of Campinas  
Campinas, Brazil  
candido@decom.fee.unicamp.br

Eduardo Rodrigues de Lima  
Hardware Dept.  
Eldorado Research Institute  
Campinas, Brazil  
eduardo.lima@eldorado.org.br

**Abstract**—This work analyzes the performance of a downlink multi-user multiple-input multiple-output (MU-MIMO) non-orthogonal multiple access (NOMA) communications system. To reduce hardware complexity and exploit antenna diversity, we consider a transmit antenna selection (TAS) scheme and equal-gain combining (EGC) receivers. Further, we consider Weibull-distributed fading channels to account for non-linearities of the propagation medium and to cover, as special cases, important fading scenarios such as Rayleigh and exponential models. Performance metrics such as the outage probability (OP) and the average bit error rate (ABER) are derived in an exact manner. An asymptotic analysis for the OP and for the ABER is also carried out. Moreover, we obtain exact expressions for the probability density function (PDF) and the cumulative distribution function (CDF) of the end-to-end signal-to-noise ratio (SNR). Interestingly, our results indicate that, except for the first user (nearest user), in a high-SNR regime the ABER achieves a performance floor that depends solely on the user's power allocation coefficient and on the type of modulation, and not on the channel statistics or the amount of transmit and receive antennas. To the best of the authors' knowledge, no performance analyses have been reported in the literature for the considered scenario. The validity of all our expressions is confirmed via Monte-Carlo simulations.

**Index Terms**—Non-orthogonal multiple access (NOMA), multi-user multiple-input multiple-output (MU-MIMO), transmit antenna selection (TAS), equal-gain combining (EGC), Weibull fading, average bit error rate (ABER), outage probability (OP).

## I. INTRODUCTION

The constant demand for massive connectivity scenarios in the sixth-generation (6G) network systems poses greater challenges than technologies such as orthogonal multiple access (OMA) can manage [1], [2]. In view of this, researchers have proposed several techniques with the potential of meeting the requirements of advanced wireless networks, such as 6G. Among them, we highlight the non-orthogonal multiple access (NOMA) technique since it (i) significantly

improves spectral and energy efficiency, (ii) provides ultra-reliable and low-latency communications (URLLC), and (iii) enables massive connectivity [3]–[8]. NOMA can be classified into two schemes: code-domain and power-domain multiplexing. In this paper, we will focus on the latter, although the same framework can be applied to the former with no substantial adjustments. The difference between NOMA and its predecessor, OMA, is that NOMA allocates time-frequency resources that are superposed and transmitted to multiple users, where for each user a specific power coefficient is allocated based on their channel conditions. On the other hand, OMA allocates resources to each user either in time, in frequency, or in code [9]. In NOMA, each receiver can decode its own information by using the method of successive interference cancellation (SIC) [3], [10], [11].

To explore power consumption reduction as well as hardware complexity and, at the same time, to improve system capacity, several works analyzed the performance of a NOMA system over different antenna configurations, e.g., single-input single-output (SISO), multiple-input single-output (MISO), single-input multiple-output (SIMO), and multiple-input multiple-output (MIMO). For instance, in [12], the authors carried out an outage probability (OP) analysis for a SISO-NOMA system in a multi-user scenario operating over  $\kappa$ - $\mu$  and  $\eta$ - $\mu$  fading environments. In [13], the authors derived an approximate closed-form solution for the OP of a SIMO-NOMA system considering equal-gain combining (EGC) receivers operating over  $\kappa$ - $\mu$  fading channels and employing the special case when  $\kappa \rightarrow 0$  (i.e., the Nakagami- $m$  fading model). The same authors proposed in [14] an approximate analysis for the OP considering a SIMO-NOMA system and employing  $\eta$ - $\mu$  fading channels, selection combining (SC), maximal-ratio combining (MRC), and EGC receivers. In [15] and [16], an analysis of performance and security for a MIMO-NOMA system using a transmit antenna selection (TAS) scheme and Rayleigh fading was presented. In [17], the authors calculated

The work of L. P. J. Jiménez was supported by Eldorado Research Institute. The work of F. D. A. García was supported by the São Paulo Research Foundation (FAPESP) under Grant 2021/03923-9.

the OP for a MIMO-NOMA system by means of Monte-Carlo simulations and employing a majority-based TAS (TAS-maj) technique, MRC receivers, and Rayleigh fading. In [18] and [19], the authors derived exact expressions for the OP, the average bit error rate (ABER), and the ergodic capacity (EC) of a SISO-NOMA system in a two-user scenario and considering  $\kappa$ - $\mu$  and shadowed  $\kappa$ - $\mu$  fading channels, respectively. Recently, in [20], the authors derived exact expressions for the OP, the ABER, and the EC for both a SISO-NOMA and MISO-NOMA (with TAS) system considering independent double Nakagami- $m$  fading channels.

According to what has been shown in the open literature, and to the best of our knowledge, no *exact* performance analysis has been carried out employing NOMA, TAS, and EGC receivers for any of the well-known fading distributions, not even for Rayleigh. This work is the first of its kind analyzing, in an exact manner, the performance of a NOMA system considering the two aforementioned diversity schemes: TAS and EGC receivers. For the analysis, we consider the Weibull fading model as it can accurately describe the non-linearities of the propagation medium in addition to encompassing, as special cases, important fading scenarios such as Rayleigh and exponential models.

The contributions of this work are summarized as follows:

- 1) Novel exact expressions for the probability density function (PDF) and cumulative distribution function (CDF) of the signal-to-noise ratio (SNR) of a MU-MIMO-NOMA system operating over independent and identically distributed (i.i.d.) Weibull fading channels.
- 2) New exact formulations for key performance metrics, namely, OP and ABER. Two important remarks are in order. Due to the versatility of the Weibull fading model, the exact OP and the ABER of MRC receivers can also be found from our analytical findings by replacing  $k$  by  $k/2$ , where  $k$  is the shape parameter of the Weibull distribution. Moreover, if we consider a single user (a non-NOMA system) and a single transmitting antenna, then our expressions provide an exact analysis in terms of OP and ABER for a SIMO system over Weibull fading channels, which so far have only been found as approximate, limited, or computationally expensive solutions [21]–[27].
- 3) Asymptotic closed-form expressions for the OP and the ABER. We show that, for the OP, the diversity order equals  $(kMN)/2$ , where  $M$  and  $N$  are the number of transmit and receive antennas, respectively. In contrast, for the ABER, the diversity order remains  $(kMN)/2$  only for the first user, while being nil for the remaining ones, with the corresponding performance floor at high SNR solely depending on the user's power allocation coefficient and the employed modulation.

The remainder of this manuscript is organized as follows. Section II introduces the MU-MIMO-NOMA system model. Section III obtains novel exact expressions for the SNR's statistics. Section IV derives exact and asymptotic expressions for

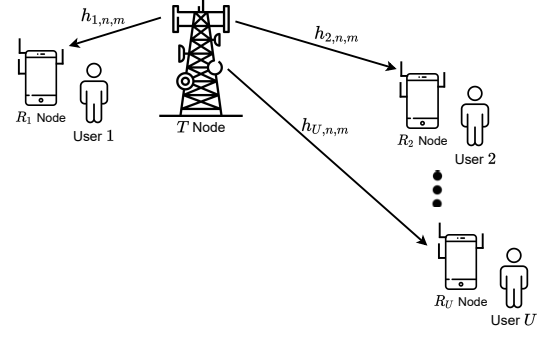


Fig. 1. Downlink MU-MIMO-NOMA system model.

the OP and the ABER. Section V discusses the representative numerical results. Finally, Section VI concludes this paper.

## II. SYSTEM MODEL

A downlink MU-MIMO-NOMA system with a single transmitter node  $T$  and multiple receiving users  $R_l$  ( $l \in \{1, 2, \dots, U\}$ ) is considered, as shown in Fig. 1. The transmitter and receiving nodes are equipped with  $M$  and  $N$  antennas, respectively. Based on NOMA principle,  $T$  simultaneously serves the multiple users over the same time and frequency resources. Users with poor channel conditions are allocated with high power coefficients, and vice-versa. The complex channel coefficient between the  $m$ -th transmitting antenna and the  $n$ -th receiving antenna of the  $l$ -th user is denoted by  $h_{l,n,m}$ . Herein, we assume that the envelope of each channel coefficient (i.e.,  $|h_{l,n,m}|$ ) follows a Weibull distribution with shape and scale parameters  $k$  and  $\lambda$ , respectively. Also, we assume that all channels experience i.i.d. fading and that perfect SIC is implemented to decode the superimposed signals [28]. Without loss of generality, we assume that  $|h_{U,n,m}| \leq \dots \leq |h_{l,n,m}| \leq \dots \leq |h_{1,n,m}|$ .<sup>1</sup> Accordingly, the users' power allocation coefficients can be sorted as  $\beta_U \geq \dots \geq \beta_l \geq \dots \geq \beta_1$ , obeying  $\sum_{j=1}^U \beta_j = 1$ .

The superimposed information signal sent by node  $T$  is given by  $s = \sum_{j=1}^U \sqrt{P_j} x_j$  where  $x_j$  is the information sent to each user,  $P_j = \beta_j P_s$  is the transmit power, and  $P_s$  is the total transmit power. To leverage the benefits of multiple antennas (i.e., to exploit antenna diversity), we employ the TAS strategy at transmission and EGC receivers at reception. Thus, the received signal at the  $l$ -th user can be written as

$$y_{l,n,m^*} = h_{l,n,m^*} \sum_{j=1}^U \sqrt{\beta_j P_s} x_j + n_{l,n}, \quad (1)$$

where  $n_{l,n}$  is the complex additive white Gaussian noise (AWGN) with zero mean and variance  $\sigma_0^2$  present at the  $n$ -th antenna of the  $l$ -th user, and  $m^*$  denotes the single antenna of node  $T$  selected for transmission according to the following criterion [30]:

$$m^* = \arg \max_{1 \leq m \leq M} \left( \sum_{n=1}^N |h_{l,n,m}| \right)^2. \quad (2)$$

<sup>1</sup>The decoding order of SIC is given by the channel ordering [29].

### III. SNR'S STATISTICS

According to (1), the instantaneous SNRs at the first (nearest user) and  $u$ -th ( $u \in \{2, 3, \dots, U\}$ ) users are respectively given by

$$\chi_1 = \frac{\beta_1 \rho \Psi_1^2}{N} \quad (3a)$$

$$\chi_u = \frac{\beta_u \rho \Psi_u^2}{N + \rho \Psi_u^2 \vartheta_u}, \quad (3b)$$

where  $\rho = P_s/\sigma_0^2$  denotes the transmit SNR,  $\vartheta_u = \sum_{j=1}^{u-1} \beta_j$ ,  $\Psi_1 = \sum_{n=1}^N |h_{1,n,m^*}|$ , and  $\Psi_u = \sum_{n=1}^N |h_{u,n,m^*}|$  with  $|h_{u,n,m^*}|$  being the independent and identically distributed (i.i.d.) Weibull fading envelopes satisfying the criterion in (2).

Taking into account that all channels undergo independent fading, the CDF of  $\Psi_u$  can be found as

$$F_{\Psi_u}(\psi_u) = \left( \Pr \left[ \sum_{n=1}^N |h_{u,n,m}| \leq \psi_u \right] \right)^M, \quad (4)$$

where  $\Pr[\cdot]$  denotes probability.

Capitalizing on [31, Proposition 1], we can rewrite (4) as

$$F_{\Psi_u}(\psi_u) = \left( \frac{k}{\lambda^k} \right)^{NM} \left( \sum_{i=0}^{\infty} \frac{\delta_i \psi_u^{ik+kN}}{\Gamma(ik + Nk + 1)} \right)^M, \quad (5)$$

where  $\Gamma(\cdot)$  is the gamma function [32, eq. (6.1.1)], and the coefficients  $\delta_i$  can be obtained recursively as

$$\delta_0 = \Gamma(k)^N \quad (6a)$$

$$\delta_i = \frac{1}{i\Gamma(k)} \sum_{p=1}^i \frac{\delta_{i-p}(-i + pN + p)\Gamma(pk + k) \left(-\left(\frac{1}{\lambda}\right)^k\right)^p}{p!}. \quad (6b)$$

From (5), we let

$$\left( \sum_{i=0}^{\infty} \psi_u^{ki} \eta_i \right)^M = \sum_{i=0}^{\infty} \psi_u^{ki} \xi_i, \quad (7)$$

in which  $\eta_i = \delta_i/\Gamma(ik + Nk + 1)$ .

Now, we make use of the following differential equation:

$$\varrho \left( \varrho^M \right)' = M \varrho^M \varrho', \quad (8)$$

where  $\varrho = \sum_{i=0}^{\infty} \psi_u^{ki} \eta_i$ ,  $\varrho^M = \sum_{i=0}^{\infty} \psi_u^{ki} \xi_i$  and the ‘‘apostrophe’’ denotes derivative with respect to  $\psi_u^k$ .

After solving (8), the coefficients  $\xi_i$  can be calculated as

$$\xi_0 = \left( \frac{\delta_0}{\Gamma(kN + 1)} \right)^M \quad (9a)$$

$$\xi_i = \frac{\Gamma(kN + 1)}{i \delta_0} \sum_{q=1}^i \frac{(-i + qM + q) \delta_q \xi_{i-q}}{\Gamma(qk + Nk + 1)}, \quad i \geq 1. \quad (9b)$$

Finally, replacing (7) and (9) into (5), we can express the CDF of  $\Psi_u$  as follows

$$F_{\Psi_u}(\psi_u) = \left( \frac{k}{\lambda^k} \right)^{NM} \sum_{i=0}^{\infty} \xi_i \psi_u^{k(i+NM)}. \quad (10)$$

Then, by taking the derivative of (10) with respect to  $\psi_u$ , one attains the PDF of  $\Psi_u$ , i.e.,

$$f_{\Psi_u}(\psi_u) = \frac{k^{NM+1}}{\psi_u} \left( \frac{\psi_u}{\lambda} \right)^{kNM} \sum_{i=0}^{\infty} \xi_i (i + NM) \psi_u^{ik}. \quad (11)$$

Using (3b), the CDF of  $\chi_u$  can be found as

$$\begin{aligned} F_{\chi_u}(\chi_u) &= \Pr \left[ \Psi_u \leq \sqrt{\frac{N\chi_u}{\rho(\beta_u - \chi_u \vartheta_u)}} \right] \\ &= F_{\Psi_u} \left( \sqrt{\frac{N\chi_u}{\rho(\beta_u - \chi_u \vartheta_u)}} \right). \end{aligned} \quad (12)$$

Then, by employing (10) and (12), the CDF of  $\chi_u$  can be finally expressed as

$$F_{\chi_u}(\chi_u) = \left( \frac{k}{\lambda^k} \right)^{NM} \sum_{i=0}^{\infty} \xi_i \left( \frac{N\chi_u}{\rho(\beta_u - \chi_u \vartheta_u)} \right)^{\frac{k}{2}(i+NM)}. \quad (13)$$

After differentiating (13) with respect to  $\chi_u$ , the PDF of  $\chi_u$  can be found as

$$\begin{aligned} f_{\chi_u}(\chi_u) &= \frac{\beta_u k^{1+NM}}{2 \chi_u (\beta_u - \chi_u \vartheta_u)} \left( \frac{1}{\lambda} \right)^{kNM} \\ &\times \sum_{i=0}^{\infty} \xi_i (i + NM) \left( \frac{N\chi_u}{\rho(\beta_u - \chi_u \vartheta_u)} \right)^{\frac{k}{2}(i+NM)}. \end{aligned} \quad (14)$$

Following a similar approach as in (13) and (14), the CDF and PDF of the SNR at the first user can be respectively obtained as<sup>2</sup>

$$F_{\chi_1}(\chi_1) = \left( \frac{k}{\lambda^k} \right)^{MN} \sum_{i=0}^{\infty} \xi_i \left( \frac{N\chi_1}{\beta_1 \rho} \right)^{\frac{k}{2}(i+MN)} \quad (15a)$$

$$f_{\chi_1}(\chi_1) = \frac{k^{MN+1}}{2 \chi_1 \lambda^{kMN}} \sum_{i=0}^{\infty} \xi_i (i + MN) \left( \frac{N\chi_1}{\beta_1 \rho} \right)^{\frac{k}{2}(i+MN)}. \quad (15b)$$

### IV. PERFORMANCE ANALYSIS

In this section, we use our derived formulations to analyze the performance of an EGC receiver subject to Weibull fading.

#### A. Outage Probability

The OPs for the first and  $u$ -th users are respectively defined as the probability that  $\chi_1$  and  $\chi_u$  fall below a specified threshold, i.e.,

$$P_{\text{out},\nu} \triangleq \Pr[\chi_\nu \leq \gamma_\nu] = F_{\chi_\nu}(\gamma_\nu), \quad (16)$$

where  $\nu \in \{1, u\}$  denotes the associated user (recall that  $u \in \{2, 3, \dots, U\}$ ).

Now, from (13) and (16), the OPs for the first and  $u$ -th users are respectively given by

$$P_{\text{out},1} = \left( \frac{k}{\lambda^k} \right)^{NM} \sum_{i=0}^{\infty} \xi_i \left( \frac{N\gamma_1}{\rho\beta_1} \right)^{\frac{k}{2}(i+NM)} \quad (17)$$

$$P_{\text{out},u} = \left( \frac{k}{\lambda^k} \right)^{NM} \sum_{i=0}^{\infty} \xi_i \left( \frac{N\gamma_u}{\rho(\beta_u - \gamma_u \vartheta_u)} \right)^{\frac{k}{2}(i+NM)}. \quad (18)$$

Moreover, we analyze the system performance in a high SNR regime (i.e., when  $\rho \rightarrow \infty$ ). Then, since the first term dominates the series in (17) and (18) (i.e., the term associated with  $i = 0$ ), the asymptotic OPs for the first and  $u$ -th users can be expressed as

$$P_{\text{out},\nu} \simeq (O_{c,\nu} \rho)^{-O_{d,\nu}}, \quad (19)$$

<sup>2</sup>As the series in (5) converges absolutely [31, Appendix], then any further manipulation or transformation over (5) will result in another absolute convergence series. The rest of the derivations follow from here.

where  $\simeq$  denotes “asymptotically equal to”;  $O_{d,1} = kMN/2$  and  $O_{d,u} = kMN/2$  are the diversity gains for the first and  $u$ -th users, respectively; and

$$O_{c,1} = \frac{\lambda^2 \beta_1}{N \gamma_1} \left( \frac{\Gamma(k+1)^N}{\Gamma(kN+1)} \right)^{-\frac{2}{kN}} \quad (20)$$

$$O_{c,u} = \frac{\lambda^2 (\beta_u - \gamma_u \vartheta_u)}{N \gamma_u} \left( \frac{\Gamma(k+1)^N}{\Gamma(kN+1)} \right)^{-\frac{2}{kN}} \quad (21)$$

are the coding gains for the first and  $u$ -th users, respectively.

### B. ABER

The ABERs for a pre-detection EGC receiver for the first and  $u$ -th users are respectively given by [33, eq. (9.61)]

$$P_{b,1} = \frac{1}{2} \int_0^\infty \operatorname{erfc} \left( \sqrt{\frac{\mathcal{A} \beta_1 \rho \psi_1^2}{N}} \right) f_{\Psi_1}(\psi_1) d\psi_1 \quad (22)$$

$$P_{b,u} = \frac{1}{2} \int_0^\infty \operatorname{erfc} \left( \sqrt{\frac{\mathcal{A} \beta_u \rho \psi_u^2}{N + \rho \psi_u^2 \vartheta_u}} \right) f_{\Psi_u}(\psi_u) d\psi_u, \quad (23)$$

in which  $\operatorname{erfc}(\cdot)$  is the complementary error function [32, eq. (7.1.2)], and  $\mathcal{A}$  is a modulation-dependent parameter. Considering the  $u$ -th user, the improper integral in (23) can be expressed in terms of the limit when  $\tau$  approaches infinity, i.e.,

$$P_{b,u} = \frac{1}{2} \lim_{\tau \rightarrow \infty} \int_0^\tau \operatorname{erfc} \left( \sqrt{\frac{\mathcal{A} \beta_u \rho \psi_u^2}{N + \rho \psi_u^2 \vartheta_u}} \right) f_{\Psi_u}(\psi_u) d\psi_u. \quad (24)$$

Replacing (11) in (24) and then changing the order of integration, we get

$$P_{b,u} = \frac{k^{NM+1}}{2} \left( \frac{1}{\lambda} \right)^{kNM} \sum_{i=0}^\infty \xi_i(i+NM) \times \lim_{\tau \rightarrow \infty} \int_0^\tau \operatorname{erfc} \left( \sqrt{\frac{\mathcal{A} \beta_u \rho \psi_u^2}{N + \rho \psi_u^2 \vartheta_u}} \right) \psi_u^{k(i+NM)-1} d\psi_u. \quad (25)$$

Finally, integrating by parts and after some algebraic manipulations with the aid of [32, eq. (4.2.1)], the ABER for the  $u$ -th user can be obtained as

$$P_{b,u} = \frac{k^{MN}}{2 \lambda^{kMN}} \sum_{i=0}^\infty \xi_i \lim_{\tau \rightarrow \infty} \left[ \tau^{k(i+MN)} \left( \operatorname{erfc}(\zeta(\tau)) + \frac{2\zeta(i,\tau)}{\sqrt{\pi}} \right) \right], \quad (26)$$

where  $\zeta(\tau)$  and  $\zeta(i,\tau)$  are auxiliary functions given by

$$\zeta(\tau) = \sqrt{\frac{\mathcal{A} \rho \tau^2 \beta_u}{N + \rho \tau^2 \vartheta_u}} \quad (27)$$

$$\zeta(i,\tau) = \sum_{j=0}^\infty \frac{\tau^{2j+1}}{j! (\varepsilon(i,j) + 1)} \left( -\sqrt{\frac{\mathcal{A} \rho \beta_u}{N}} \right)^j \times {}_2F_1 \left( j + \frac{3}{2}, \frac{\varepsilon(i,j) + 1}{2}; \frac{\varepsilon(i,j) + 3}{2}; -\frac{\tau^2 \vartheta_u}{N \rho^{-1}} \right), \quad (28)$$

in which  $\varepsilon(i,j) = 2j + ik + kMN$  and  ${}_2F_1(\cdot, \cdot; \cdot; \cdot)$  is the Gauss hypergeometric function [34, Eq. (15.1.1)].

<sup>3</sup>It is worth noting that  $\operatorname{erfc}(\cdot)$  and  ${}_2F_1(\cdot, \cdot; \cdot; \cdot)$  can be quickly and efficiently evaluated in any mathematical software.

To ease the numerical calculation, (26) can be accurately approximated as

$$P_{b,u} \approx \frac{k^{MN}}{2 \lambda^{kMN}} \sum_{i=0}^\infty \xi_i (a^\dagger)^{k(i+MN)} \left( \operatorname{erfc}(\zeta_{(a^\dagger)}) + \frac{2\zeta(i,a^\dagger)}{\sqrt{\pi}} \right), \quad (29)$$

where  $a^\dagger$  is an accuracy-dependent parameter. The higher the values of  $a^\dagger$ , the higher the accuracy. A value of  $a^\dagger = 35$  guarantees a relative error of less than  $10^{-6}$ , as will be seen in Section V.

Following the same derivation steps as in (26), the exact ABER for the first user can be obtained as

$$P_{b,1} = \frac{k^{MN}}{2 \sqrt{\pi} \lambda^{kMN}} \sum_{i=0}^\infty \frac{\xi_i \Gamma\left(\frac{ik+kMN+1}{2}\right)}{\left(\frac{\mathcal{A} \beta_1 \rho}{N}\right)^{\frac{k}{2}(i+MN)}}. \quad (30)$$

An asymptotic ABER for the first user can also be found by using the first term in (30), resulting in

$$P_{b,1} \simeq (G_{c,1} \rho)^{-G_{d,1}}, \quad (31)$$

where  $G_{d,1} = kMN/2$  is the diversity gain and

$$G_{c,1} = \frac{\mathcal{A} \beta_1 \lambda^2}{N} \left[ \left( \frac{\Gamma\left(\frac{kMN+1}{2}\right)}{2\sqrt{\pi}} \right)^M \frac{\Gamma(k+1)^N}{\Gamma(kN+1)} \right]^{-\frac{2}{kN}} \quad (32)$$

is the coding gain. It is important to highlight that all exact expressions derived herein converge rapidly (i.e., with few summation terms) and are new in the literature.

1) *Minimum Achievable ABER for the  $u$ -th user:* Using a partial fraction decomposition into (3b), we obtain

$$\chi_u = \frac{\mathcal{A} \beta_u}{\vartheta_u} - \frac{\mathcal{A} N \beta_u}{\vartheta_u (N + \rho \Psi^2 \vartheta_u)}. \quad (33)$$

Noticing that in the high SNR regime (i.e., when  $\rho \rightarrow \infty$ ), the second term vanishes. Then, an asymptotic expression for the SNR can be obtained as

$$\chi_u \simeq \frac{\mathcal{A} \beta_u}{\vartheta_u}. \quad (34)$$

Finally, substituting (34) into (23), a minimum achievable ABER (i.e., a performance floor at high SNR) for the  $u$ -th user can be found as

$$P_{b,u}^{\min} = \frac{1}{2} \operatorname{erfc} \left( \sqrt{\frac{\mathcal{A} \beta_u}{\vartheta_u}} \right). \quad (35)$$

Notice that the minimum achievable ABER for the  $u$ -th user is independent of the channel statistics (e.g., the type of fading) and the number of antennas in the diversity schemes (e.g., EGC, MRC, and TAS). Indeed, it only depends on the user's power allocation coefficient and the type of modulation.

## V. NUMERICAL RESULTS

In this section, we corroborate our analytical findings through Monte-Carlo simulations.<sup>4</sup>

Fig. 2 shows the OP in terms of the SNR for various values of shape parameter  $k$ . The figure indicates that for the first and  $u$ -th user, the system performance improves as  $k$  increases and

<sup>4</sup>The number of Monte-Carlo realizations was set to  $10^7$ . Also, we used a maximum of 200 terms in our derived series.

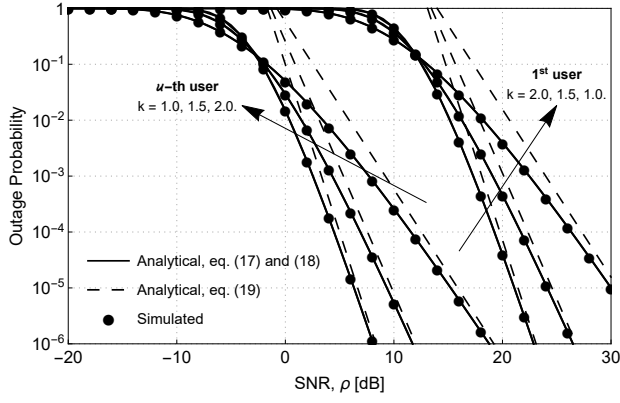


Fig. 2. OP versus SNR using  $\lambda = 2$ ,  $N = 2$ ,  $M = 3$ ,  $\gamma_u = 0$ ,  $\beta_u = 0.65$ ,  $\beta_1 = 0.01$ ,  $\vartheta_u = 0.35$ , and various values of  $k$ .

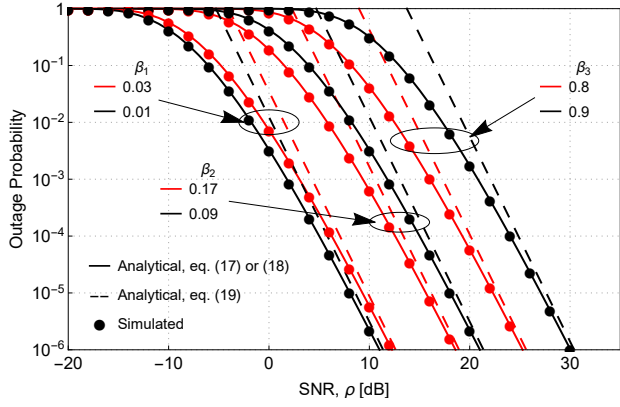


Fig. 3. OP versus SNR using  $k = 1.2$ ,  $\lambda = 2$ ,  $N = 2$ ,  $M = 3$ ,  $\gamma_u = 0$ , and various values of  $\beta_u$ . This corresponds to two scenarios having three users each with power allocation coefficients  $\beta_1$ ,  $\beta_2$ , and  $\beta_3$ .

deteriorates otherwise. The number of transmitting and receiving antennas,  $N$  and  $M$ , also improves the system's reliability. However, the figures varying the number of antennas were omitted here due to space limitations. The beneficial effects of increasing  $k$ ,  $N$ , or  $M$  is because the system's diversity order is equal to  $(kNM)/2$ .

Fig. 3 shows the OP in terms of the SNR for two scenarios (curves in red for the first scenario and curves in black for the second scenario) with three different values of  $\beta_u$  (i.e., three users). More precisely, Fig. 3 highlights the impact of the power allocation factor  $\beta$  in a MU-MIMO-NOMA system. Since the majority of the power is allocated to the most distant user, lower SNR values are needed to achieve a high performance in terms of OP, as expected. Then, it is straightforward to see that the second user is placed in middle ground in terms of performance and that the nearest user shows the worst performance due to the low power coefficient assigned. Here, the importance of correct power allocation in NOMA systems is evidenced.

Fig. 4 depicts the ABER for multiple values of  $k$  for the  $u$ -th and first user. For the  $u$ -th the figure indicates that higher values of the shape parameter  $k$  lead to higher values of

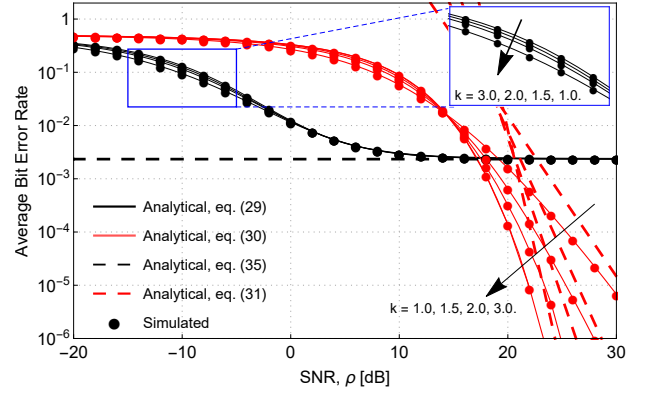


Fig. 4. ABER versus SNR using  $\lambda = 2$ ,  $N = 2$ ,  $M = 3$ ,  $\mathcal{A} = 1$ ,  $\beta_u = 0.8$ ,  $\vartheta_u = 0.2$ ,  $\beta_1 = 0.01$  and various values of  $k$ .

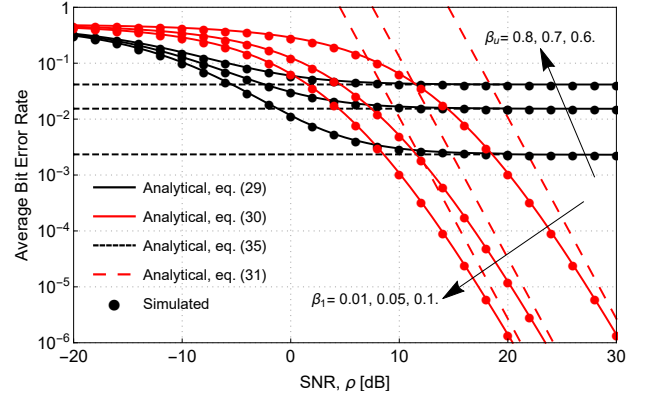


Fig. 5. ABER versus SNR using  $k = 1.2$ ,  $\lambda = 2$ ,  $N = 2$ ,  $M = 3$ ,  $\mathcal{A} = 1$ ,  $\vartheta_u = 1 - \beta_u$  and various values of  $\beta_u$  and  $\beta_1$ .

ABER, which deteriorates the system performance. For the first user the opposite occurs, i.e., as  $k$  increases better ABER values are reached. Also, notice that regardless of the values of  $k$ , at high SNR regime the ABER reaches the minimum value (performance floor), given in (35) (the same occurs for different values of the scale parameter  $\lambda$ , omitted here due to space constraints). That is, the minimum ABER is independent of the fading parameters. Moreover, for the  $u$ -th user, the figure also shows that for  $k > 1$  the ABER curves almost overlapped. Therefore, in scenarios where the fading channel follows a Weibull distribution with shape parameter  $k > 1$ , an analytical (or simulated) ABER analysis can be simplified (or approximated) by considering  $k = 2$ , i.e., Rayleigh fading.

Fig. 5 shows the ABERs for different values of  $\beta_1$  and  $\beta_u$ . In particular, for the first user, it can be noticed that as the SNR increases the ABER decreases. On the other hand, for the  $u$ -th user, it can be seen that at high SNR, the ABER reaches a performance floor that depends on the power coefficients. Notice how the system improves as the power coefficients increase, i.e., the higher the power coefficient, the smaller the ABER. Also, notice the influence of the power coefficient parameters in the ABER, where higher  $\beta_1$  and  $\beta_u$  values produce smaller ABER values.

Finally, notice the perfect agreement between Monte-Carlo simulations and our analytical results, thereby corroborating our findings. Moreover, notice how our asymptotic formulations provide excellent fits in the high-SNR regime.

## VI. CONCLUSION

This work analyzed the performance of a MU-MIMO-NOMA system operating over Weibull fading channels. Exact formulations for the SNR's statistics, OP, and ABER were provided. An asymptotic analysis was also carried out to show how the physical parameters roughly affect the system performance. Analytical and numerical results indicate that the system performance improves as  $k$ ,  $M$ , or  $N$  increases. Moreover, it was shown that the minimum achievable ABER for the  $u$ -th user is independent of the fading scenario and of the number of antennas in the diversity schemes. In fact, it only depends on the user's power allocation coefficient and the type of modulation.

## REFERENCES

- [1] Y. L. Lee, D. Qin, L.-C. Wang, and G. H. Sim, "6G massive radio access networks: Key applications, requirements and challenges," *IEEE Open J. Veh. Technol.*, vol. 2, pp. 54–66, Dec. 2021.
- [2] M. Aldababsa, M. Toka, S. Gökçeli, G. K. Kurt, and O. Kucur, "A tutorial on nonorthogonal multiple access for 5G and beyond," *Wireless Communications and Mobile Computing*, vol. 2018, 2018.
- [3] S. M. R. Islam, N. Avazov, O. A. Dobre, and K.-s. Kwak, "Power-domain non-orthogonal multiple access (NOMA) in 5G systems: Potentials and challenges," *IEEE Commun. Surveys Tuts.*, vol. 19, no. 2, pp. 721–742, Oct. 2017.
- [4] K. Yang, N. Yang, N. Ye, M. Jia, Z. Gao, and R. Fan, "Non-orthogonal multiple access: Achieving sustainable future radio access," *IEEE Commun. Mag.*, vol. 57, no. 2, pp. 116–121, Nov. 2019.
- [5] M. Amjad and L. Musavian, "Performance analysis of NOMA for ultra-reliable and low-latency communications," in *IEEE Globecom Workshops (GC Workshops)*, Feb. 2018, pp. 1–5.
- [6] R. Rai, H. Zhu, and J. Wang, "Performance analysis of NOMA enabled fog radio access networks," *IEEE Trans. Commun.*, vol. 69, no. 1, pp. 382–397, Oct. 2021.
- [7] S. Mounchili and S. Hamouda, "Pairing distance resolution and power control for massive connectivity improvement in NOMA systems," *IEEE Trans. Veh. Technol.*, vol. 69, no. 4, pp. 4093–4103, Feb. 2020.
- [8] C. B. Mwakwata, O. Elgarhy, M. M. Alam, Y. Le Moullec, S. Päränd, K. Trichias, and K. Ramantas, "Cooperative scheduler to enhance massive connectivity in 5G and Beyond by minimizing interference in OMA and NOMA," *IEEE Syst. J.*, pp. 1–12, Oct. 2021.
- [9] J. Cheon and H.-S. Cho, "Power allocation scheme for non-orthogonal multiple access in underwater acoustic communications," *Sensors*, vol. 17, no. 11, 2017.
- [10] Z. Chen, Z. Ding, X. Dai, and R. Zhang, "An optimization perspective of the superiority of NOMA compared to conventional OMA," *IEEE Trans. Signal Process.*, vol. 65, no. 19, pp. 5191–5202, Jul. 2017.
- [11] Z. Ding, Y. Liu, J. Choi, Q. Sun, M. Elkashlan, I. Chih-Lin, and H. V. Poor, "Application of non-orthogonal multiple access in LTE and 5G networks," *IEEE Commun. Mag.*, vol. 55, no. 2, pp. 185–191, Feb. 2017.
- [12] P. Sharma, A. Kumar, and M. Bansal, "Performance analysis of downlink NOMA over  $\eta - \mu$  and  $\kappa - \mu$  fading channels," *IET Communications*, vol. 14, no. 3, pp. 522–531, 2020.
- [13] —, "On performance of downlink NOMA with equal gain combining over  $\kappa - \mu$  fading channel for limiting value of  $\kappa$ ," in *Proc. IEEE 4th Conf. Inf. Commun. Technol. (CICT)*, Dec. 2020, pp. 1–6.
- [14] —, "Performance analysis of downlink NOMA system with diversity combining schemes over  $\eta - \mu$  fading channel," *Phys. Commun.*, vol. 47, p. 101383, 2021.
- [15] A. P. Shrestha, T. Han, Z. Bai, J. M. Kim, and K. S. Kwak, "Performance of transmit antenna selection in non-orthogonal multiple access for 5G systems," in *Proc. 8th Int. Conf. Ubiquitous Future Ntw.*, Jul. 2016, pp. 1031–1034.
- [16] N.-L. Nguyen, H.-N. Nguyen, N.-T. Nguyen, D.-T. Do, A.-T. Le, M. Voznak, and J. Zdravlek, "On secure cognitive radio networks with NOMA: Design of multiple-antenna and performance analysis," in *Proc. IEEE Microw. Theory Techn. Wireless Commun.*, vol. 1, Nov. 2020, pp. 1–6.
- [17] M. Aldababsa and O. Kucur, "Outage performance of NOMA with majority based TAS/MRC scheme in Rayleigh fading channels," in *Proc. 27th Signal Process. Commun. Appl. Conf. (SIU)*, Aug. 2019, pp. 1–4.
- [18] A. Alqahtani, E. Alsusa, A. Al-Dweik, and M. Al-Jarrah, "Performance analysis for downlink NOMA over  $\alpha - \mu$  generalized fading channels," *IEEE Trans. Veh. Technol.*, vol. 70, no. 7, pp. 6814–6825, May 2021.
- [19] B. M. ElHalawany, F. Jameel, D. B. da Costa, U. S. Dias, and K. Wu, "Performance analysis of downlink NOMA systems over  $\kappa - \mu$  shadowed fading channels," *IEEE Trans. Veh. Technol.*, vol. 69, no. 1, pp. 1046–1050, Jan. 2021.
- [20] N. Jaiswal and N. Purohit, "Performance analysis of NOMA-enabled vehicular communication systems with transmit antenna selection over double Nakagami- $m$  fading," *IEEE Trans. Veh. Technol.*, vol. 70, no. 12, pp. 12 725–12 741, Dec. 2021.
- [21] D. G. Brennan, "Linear diversity combining techniques," *Proc. IRE*, vol. 47, pp. 1075–1102, Jun. 1959.
- [22] N. C. Beaulieu, "An infinite series for the computation of the complementary probability distribution function of a sum of independent random variables and its application to the sum of Rayleigh random variables," *IEEE Trans. Commun.*, vol. 38, no. 9, pp. 1463–1474, Sep. 1990.
- [23] G. Karagiannidis, D. Zogas, N. Sagias, S. Kotsopoulos, and G. Tombras, "Equal-gain and maximal-ratio combining over nonidentical Weibull fading channels," *IEEE Trans. Wireless Commun.*, vol. 4, no. 3, pp. 841–846, May 2005.
- [24] M. Ismail and M. Matalgah, "Performance of dual maximal ratio combining diversity in nonidentical correlated Weibull fading channels using Pade/spl acute/ approximation," *IEEE Tran. Commun.*, vol. 54, no. 3, pp. 397–402, Mar. 2006.
- [25] T. Chaayra, F. E. Bouanani, and H. Ben-azza, "Performance analysis of TAS/MRC based MIMO systems over Weibull fading channels," in *Proc. Int. Conf. Advanced Commun. Syst. Inf. Security (ACOSIS)*, Feb. 2016, pp. 1–6.
- [26] M. Bilim, "Approximate ASER analysis of MIMO TAS/MRC networks over Weibull fading channels," *Ann. Telecommun.*, vol. 76, no. 1, pp. 73–81, 2021.
- [27] Q. T. Zhang, "Error rates for 4-branch equal-gain combining in independent Rayleigh fading: A simple explicit solution," *IEEE Commun. Lett.*, vol. 26, no. 2, pp. 269–272, Feb. 2022.
- [28] J. Liberti, S. Moshavi, and P. Zablocky, "Successive interference cancellation," *US Patent 8670418 B*, vol. 2, 2014.
- [29] T. Hou, X. Sun, and Z. Song, "Outage performance for non-orthogonal multiple access with fixed power allocation over Nakagami- $m$  fading channels," *IEEE Commun. Lett.*, vol. 22, no. 4, pp. 744–747, Apr. 2018.
- [30] J. M. Moualeu, D. B. da Costa, F. J. Lopez-Martinez, W. Hamouda, T. M. N. Nkouatchah, and U. S. Dias, "Transmit antenna selection in secure MIMO systems over  $\alpha - \mu$  fading channels," *IEEE Trans. Commun.*, vol. 67, no. 9, pp. 6483–6498, Sep. 2019.
- [31] F. D. A. García, F. R. A. Parente, G. Fraidenraich, and J. C. S. S. Filho, "Light exact expressions for the sum of Weibull random variables," *IEEE Wireless Commun. Lett.*, vol. 10, no. 11, pp. 2445–2449, Nov. 2021.
- [32] M. Abramowitz and I. A. Stegun, *Handbook of Mathematical Functions with Formulas, Graphs, and Mathematical Tables*, 10th ed. Washington, DC: US Dept. of Commerce: National Bureau of Standards, 1972.
- [33] M. K. Simon and M.-S. Alouini, *Digital communication over fading channels*, 2nd ed. Hoboken: NJ: Wiley, 2004.
- [34] F. W. J. Olver, D. W. Lozier, R. F. Boisvert, and C. W. Clark, *NIST Handbook of Mathematical Functions*, 1st ed. Washington, DC: US Dept. of Commerce: National Institute of Standards and Technology (NIST), 2010.